Do Low-Coordinated Group 1-3 Cations $M^{n+}L_m$ (M^{n+} = K^+, Rb^+, Cs^+, Ca^{2+}, Sr^{2+}, Ba^{2+}, Sc^{3+}, Y^{3+}, La^{3+}; L = NH_3, H_2O, HF; m = 1-3) with a Formal Noble-Gas Electron Configuration Favor Regular or "Abnormal" Shapes?

Martin Kaupp and Paul v. R. Schleyer*

Institut für Organische Chemie I, Friedrich-Alexander Universität Erlangen-Nürnberg, Henkestrasse 42, D-8520 Erlangen, Germany *(Received: May 11, 1992)*

The equilibrium structures of the complexes $M^{n+}L_m$ (M^{n+} = K^+, Rb 1+, Cs^+, Ca^{2+}, Sr^{2+}, Ba^{2+}, Sc^{3+}, Y^{3+}, La^{3+}; L = NH_3, H_2O, HF; m = 1-3) have been computed ab initio by using quasirelativistic pseudopotentials and flexible, polarized basis sets. Many of these species do not obey expectations based on the valence shell electron pair repulsion (VSEPR) rules or simple electrostatic models. For m = 2 (except for K^+) bent L-M-L arrangements are favored energetically over linear structures. The energy gain upon bending increases along the series M^{n+} = K^+, Rb^+, Ca^{2+}, Cs^+, Sr^{2+}, Ba^{2+}, Sc^{3+}, Y^{3+}, La^{3+}. The smallest angles (ca. 110°) and largest linearization energies (up to ca. 7 kcal/mol for $La^{3+}(NH_3)_2$) are found with Ba^{2+}, Sc^{3+}, Y^{3+}, and La^{3+}. Complexes of Ba^{2+} and La^{3+} with three NH_3, H_2O, or HF ligands exhibit a preference for pyramidal over trigonal-planar arrangements although the pyramidalization energy is less than 1 kcal/mol. While the main reason for the very small bending effects in the group 1 cations is the polarization of the cation by the field of the ligands, the participation of d orbitals in covalent bonding contributions seems to be the major driving force for the group 3 cations. Both effects probably are important for the group 2 cations. The observed angles in the $M^{n+}L_2$ complexes are considerably smaller than those for the alkaline-earth metal dihalides, dihydroxides, or diamides; $La^{3+}(HF)_3$ is more pyramidal than LaF_3. These smaller angles are due to decreased repulsion between neutral ligands as compared to anions and to reduced π-bonding in the cationic complexes. Extended d-basis sets are needed for the computation of heavy alkaline-earth metal cations. In particular, model ab initio calculations used previously to parametrize semiempirical force fields for calcium protein simulations suffered from the use of inadequate Ca basis sets.

Introduction

What are the equilibrium structures of cationic d^0 metal complexes such as $Ba^{2+}(H_2O)_2$ and $Ba^{2+}(H_2O)_3$? Recent computational studies of various alkaline-earth metal MX_2 compounds[1-6] established that some of these neutral species prefer bent structures (particularly significant for BaX_2 compounds such as $BaMe_2$[4] or BaF_2[2-4]). Other MX_2 compounds either are linear or exhibit extremely floppy "quasilinear"[2] behavior. These ab initio results confirmed the early experimental work of Klemperer and coworkers[7] and settled a long-standing dispute about the "abnormal shapes"[8] for these species. Such nonlinear structures violate the usual predictions in main-group structural chemistry,[9] e.g., valence shell electron pair repulsion (VSEPR)[9b] or simple electrostatic models would lead one to expect linear arrangements.

Two major factors favor bent structures: The participation of metal d orbitals in the small covalent σ-bonding contributions (i.e., the d_{yz} orbital for the X-M-X angle in the yz plane) and the polarization of the metal subvalence shell by the field of the ligands.[1,3] Of course, the mutual repulsion of the X^- anions opposes bending.[3,10] When the substituents are π-donors (e.g., X = F, NH_2,[4] η_5-C_5H_5[5]), π-bonding contributions also favor linear geometries.[4-6,11]

An extension of these concepts to tricoordinated species led us to consider pyramidal structures for d^0 MX_3 species. Indeed, ScH_3 seems to be pyramidal,[11] and there exist several X-ray structures indicating pyramidal ScX_3 or LnX_3 (Ln = Eu, Nd; X = N($SiMe_3$)$_2$) arrangements.[12] On the other hand, ScF_3 and YF_3 are genuinely planar.[11,13a,b] Even LaF_3, the most likely candidate for a pyramidal d^0 metal trihalide structure (largest rare-earth metal trication, smallest halide anion), has a planarization barrier of less than 0.2 kcal/mol.[13c] This is due to π-bonding contributions which favor planar structures.[11] Moreover, the maximum X-M-X angle for a symmetrical MX_3 system is only 120° (compared to 180° for MX_2 species). Thus, anion-anion repulsion is severe.

Neutral ligands should exhibit less ligand-ligand repulsion and also reduced π-bonding. However, σ-contributions and cation polarization, i.e., the factors that favor bent (pyramidal) structures, also may be expected to be smaller with neutral ligands. Complexes of cations of electropositive metals with neutral ligands like H_2O or NH_3 are important for cation solvation[14] and also for many atmospheric and surface processes.[15] Experimental gas-phase binding enthalpies for the alkali-metal monocations to water molecules, one to six, have been determined by Dzidič and Kebarle using high-pressure mass spectrometry.[16] These energies and a simple electrostatic model were employed to estimate the M-O distances. Castleman et al. determined the corresponding NH_3 binding enthalpies.[17] The study of $M^{2+}\cdot L_m$ clusters in the gas phase is more difficult,[18] and no data on low-coordinated species (m < 6) have been reported. Gas-phase data for complexes of triply charged cations are not available either. While the mass spectrometry experiments yield important thermodynamic (and sometimes kinetic) data, only limited information concerning structures is provided.

Earlier theoretical studies have mainly dealt with complexes of the lighter group 1, 2, and 13 cations Li^+, Na^+, Be^{2+}, Mg^{2+}, and Al^{3+}.[19] Computational data involving the heavier metals are less abundant. The single-ligand complexes $M^{n+}\cdot H_2O$ and $M^{n+}\cdot NH_3$ (M^{n+} = K^+, Rb^+, Ca^{2+}, Sr^{2+}, Sc^{3+}) have been computed at the Hartree-Fock level of theory.[20-32] Due to the importance of Ca^{2+} in biological systems, many studies on Ca^{2+}-water complexes and other model systems have been performed.[23-33] A common aim of these model investigations on small systems was to obtain potential energy functions to be used in molecular dynamics or Monte Carlo simulations of larger clusters. However, almost all ab initio calculations performed on Ca^{2+}-neutral ligand systems (and also for Sr^{2+} species) have employed inadequate metal basis sets, lacking sufficient d-functions (for a discussion, see section A). No information on complexes of Ba^{2+}, Y^{3+}, or La^{3+} with neutral ligands is available. Bauschlicher and coworkers have studied the complexes of transition-metal monocations with one and two neutral ligands extensively[34] and have investigated the $M^+\cdot(H_2O)_m$ ($m \le 4$) sets with M^+ = Mg^+, Al^+.[35] After completing this study, we received a preprint of related work by Bauschlicher et al.[36] This group studied the complexes of Ca^{2+} and Sr^{2+} with two or three water molecules using extended basis sets. Their findings will be compared to our results below.

Will dicoordinate cation-neutral complexes favor bent or linear structures? Will tricoordinate complexes such as $Ba^{2+}(H_2O)_3$ be planar or pyramidal? Which electronic factors control the structures of these species? To provide answers, we have carried

0022-3654/92/2096-7316$03.00/0

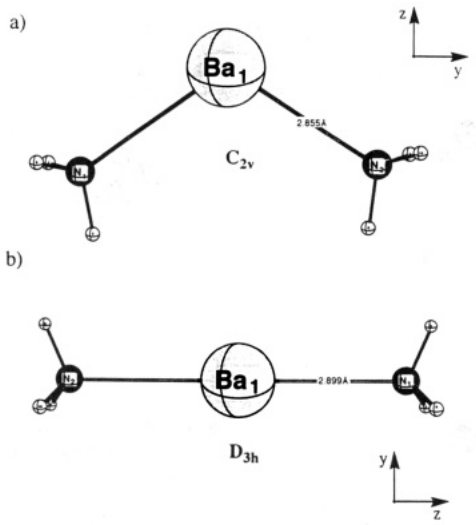

Figure 1. $M^{n+}(NH_3)_2$ geometries, illustrated with M = Ba^{2+}: (a) bent C_{2v} structure; (b) linear D_{3h} structure.

out ab initio geometry optimizations with extended basis sets (sometimes also including electron correlation corrections) for a variety of complexes of K^+, Rb^+, Cs^+, Ca^{2+}, Sr^{2+}, Ba^{2+}, Sc^{3+}, Y^{3+}, and La^{3+} with the neutral ligands NH_3, H_2O, and HF.

Computational Details

We employed quasirelativistic energy-adjusted pseudopotentials treating K, Rb, and Cs as 9-valence-electron,[37] Ca, Sr, and Ba as 10-valence-electron,[1] and Sc[38], Y[39], and La[40] as 11-valence-electron systems (for La, the f-projector ensures a $4f^0$ core occupation[40]). Valence 7s5p-basis sets,[37] augmented by two diffuse p-polarization sets[41] and by two d-functions[41] have been used for K, Rb, and Cs. The 6s6p5d-basis sets for Ca, Sr, and Ba[1] have been employed in our previous studies of alkaline-earth-metal MX_2 compounds.[1,3-6] Most of the Hartree-Fock geometry optimizations were carried out with a 6s6p2d contraction.[1] Post-Hartree–Fock (MP2, MP4) computations used the uncontracted group 2 basis sets augmented by one f-function.[1] A valence [8s7p6d]/(6s5p4d)-basis for Sc[38] and [7s6p5d]/(5s4p3d) sets for Y[39] and La[40] were employed at the SCF level. One f-function with exponents α = 1.54 (Sc), 0.95 (Y), and 0.486 (La)[40] has been added in post-SCF calculations.

Single-electron-fit pseudopotentials for N and O[42] and a multielectron-fit pseudopotential for F[43] replace the He core of these three elements. The corresponding 4s4p-valence bases[3,44] have been contracted to double-ζ (DZ) quality and augmented by a diffuse sp-set[3,45] and one d-polarization function.[41] Dunning and Hay's [4s1p]/(2s1p) hydrogen basis[46] was used. The hydrogen p-functions were omitted for the three-ligand complexes.

Symmetry restrictions have been applied to the full geometry optimizations: A planar C_{2v} geometry was imposed for $M^{n+}(H_2O)$ and C_{3v} symmetry for $M^{n+}(NH_3)$ (cf. section A). The complexes $M^{n+}(NH_3)_2$ were optimized within D_{3d} (linear L–M–L arrangement) and C_{2v} symmetry (bent structure), respectively (cf. Figure 1). While these are probably transition states with respect to M–NH_3 rotation, the barriers are expected to be negligible (cf. the isoelectronic $M(CH_3)_2$ species, M = Ca, Sr, Ba[4]). At the Hartree–Fock level, several conformations have been considered for the diaquo complexes (cf. Figure 2). MP2 optimizations were restricted to linear D_{2h} (cf. Figure 2f) and bent C_{2v}^{op} (with the hydrogen atoms out-of-plane, cf. Figure 2c) structures. $La^{3+}(HF)_2$ was optimized within C_{2h} and C_2 symmetries. Figure 3 displays four of the six structures examined for $M^{n+}(H_2O)_3$ complexes (M^{n+} = Ba^{2+}, La^{3+}). The two possible D_{3h} structures also have been optimized. Figure 4 shows the two geometries studied for $La^{3+}(NH_3)_3$. $La^{3+}(HF)_3$ was optimized in D_{3h} and C_{3v} symmetry.

All calculations have been performed with the GAUSSIAN 88[47] and GAUSSIAN 90[48] programs. Natural population analyses (NPA)[49] employed the Gaussian adaptations of the Reed/Weinhold NBO program.

TABLE I: MO and OH Distances (Å) and H–O–H Angles (deg) for $M^{n+}H_2O$[a]

M^{n+}	R–MO	R–OH	H–O–H
K^+	2.649 (2.621)[b]	0.944 (0.963)	105.6 (104.0)
Rb^+	2.842 (2.807)[b]	0.944 (0.962)	105.6 (103.8)
Cs^{1+}	3.044 (2.998)[b]	0.944 (0.962)	105.6 (103.8)
Ca^{2+}	2.276 (2.252)[c]	0.954 (0.972)	104.4 (103.5)
Sr^{2+}	2.453 (2.423)[c]	0.952 (0.971)	104.2 (103.2)
Ba^{2+}	2.663 (2.620)[c]	0.951 (0.970)	104.2 (102.9)
Sc^{3+}	1.973 (1.939)[d]	0.984 (1.010)	103.0 (103.0)
Y^{3+}	2.201 (2.154)[d]	0.972 (0.994)	103.0 (102.2)
La^{3+}	2.408 (2.369)[d]	0.967 (0.988)	102.6 (102.0)
free H_2O		0.940 (0.959)	106.7 (104.7)

[a] Hartree–Fock results with MP2 geometries in parentheses. Optimization imposing C_{2v} symmetry. [b] Empirical calculations based on experimental gas-phase binding enthalpies and a simple electrostatic model yield M–O distances of 2.60, 2.76, and 2.98 Å for M = K, Rb, Cs, respectively (ref 16). [c] Uncontracted 6s6p5d1f metal basis sets used for MP2 optimizations. [d] One f-function added in MP2 calculations.

TABLE II: MN and NH Distances (Å) and H–N–H Angles (deg) for $M^{n+}NH_3$[a]

M^{n+}	R–MN	R–NH	H–N–H
K^+	2.821	1.002	105.8
Rb^+	3.023	1.002	105.9
Cs^+	3.226	1.001	106.2
Ca^{2+}	2.423	1.010	103.8
Sr^{2+}	2.604	1.009	103.8
Ba^{2+}	2.815	1.007	104.0
Sc^{3+}	2.106	1.031	102.7
Y^{3+}	2.341	1.023	102.6
La^{3+}	2.551	1.019	102.5
free NH_3		0.997	110.0

[a] Hartree–Fock results.

Results and Discussion

(A) Geometries and Electronic Structures. (*a*) *Single-Ligand Complexes.* The single-ligand complexes do not offer any structural alternatives to those geometries expected from simple electrostatic considerations. Harmonic frequency calculations for $Ca^{2+}(H_2O)$ and $Sc^{3+}(H_2O)$ (the details are available as supplementary material; see paragraph at end of paper) confirm that $M^{n+}(H_2O)$ complexes quite generally prefer a planar C_{2v} structure;[27] the ammonia complexes exhibit C_{3v} symmetry. We have included the single-ligand systems for comparison (in particular to previous investigations) and to obtain the first-ligand binding energies (cf. section B). Tables I and II list the geometry parameters for the water and ammonia complexes, respectively (and for the free ligands). The effect of electron correlation on the structures of the hydrate complexes has been considered at the MP2 level of theory.

In several cases comparisons with previous theoretical studies are possible: The Hartree–Fock K–O distance in $K^+(H_2O)$ is in reasonable agreement with previous calculations.[20-22,27] The HF Sc–O distance in $Sc^{3+}(H_2O)$ is slightly (ca. 2 pm) shorter than that found by Davy and Hall.[27] The M–O and M–N distances obtained by Hofmann et al.[29] generally are shorter (ca. 3–10 pm) than our Hartree–Fock values for K^+, Rb^+, and Sc^{3+}. Significant basis set superposition errors (BSSE) due to the rather small ligand basis sets are responsible for their short distances. Hofmann et al.'s M–L distances for the Ca^{2+} and Sr^{2+} complexes[29] are in much better agreement with our HF results. However, this is due to an accidental cancellation of errors in their calculations: While inadequately small N and O basis sets lead to short distances, the omission of d-functions on Ca and Sr causes errors in the other direction (see below).

Our Hartree–Fock M–O distance of 2.276 Å for $Ca^{2+}(H_2O)$ is considerably shorter than those obtained in previous studies (2.40,[22] 2.40–2.41,[25] 2.34,[27] 2.395,[28] 2.329 Å[32]) except for those cases, where too small ligand basis sets lead to large BSSE.[21,28,29] Why Krauss and Stevens[31] obtain a Ca–O distance of 2.256 Å

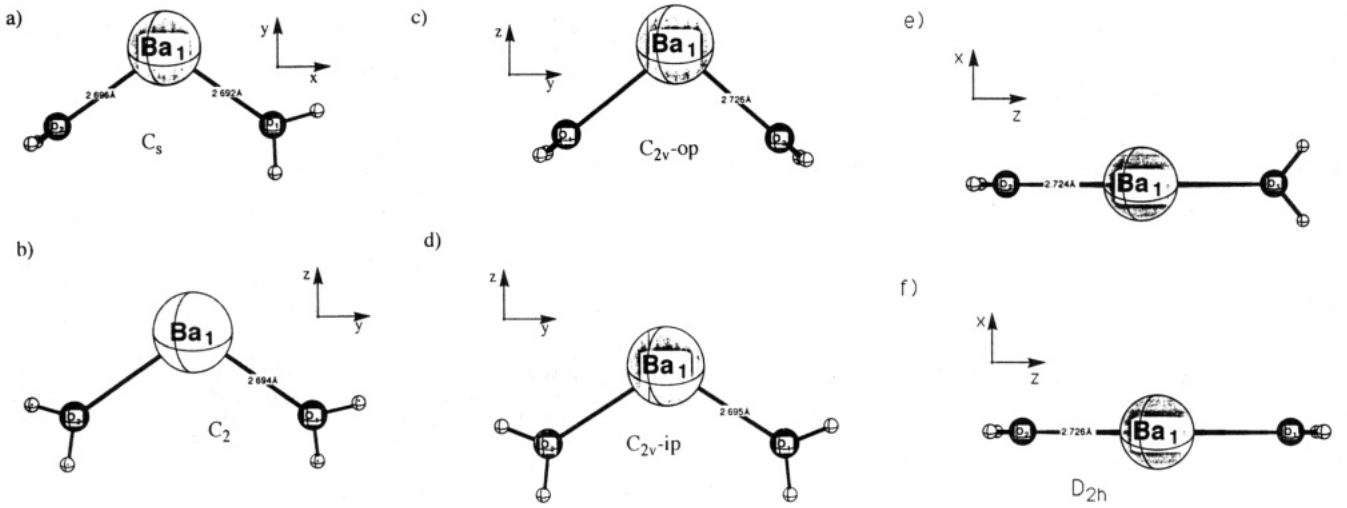

Figure 2. $M^{n+}(H_2O)_2$ geometries, illustrated with M = Ba^{2+}. Coordinate axes indicate the standard orientations for the different point groups. These serve as a basis for orbital designations. (a) C_s. (b) C_2. (c) Out-of-plane C_{2v}, C_{2v}(op). (d) In-plane C_{2v}, C_{2v}(ip). (e) D_{2d}. (f) D_{2h}.

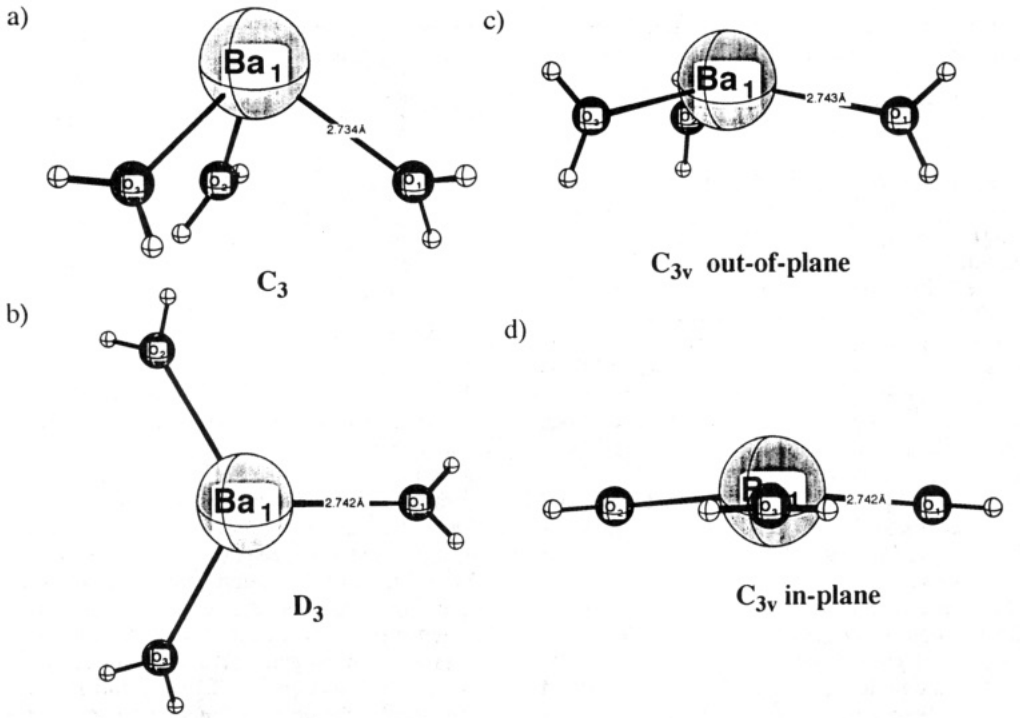

Figure 3. $M^{n+}(H_2O)_3$ geometries, illustrated with M = Ba^{2+}. (a) C_3. (b) Planar D_3. (c) Out-of-plane C_{3v}. (d) In-plane C_{3v}.

in their calculations with a two-valence-electron pseudopotential and a shared-exponent 31-sp-basis is not completely clear. Their pseudopotential parametrization seems to be responsible for the small distance. In all of the above cases, no or only one diffuse d-function has been used for the metal. Only the very recent study of Bauschlicher et al.[36] employed large d–basis sets for Ca^{2+} and Sr^{2+}. Their M–O distances (2.275 Å in $Ca^{2+}(H_2O)$ and 2.452 in $Sr^{2+}(H_2O)$) agree excellently with our HF results (cf. Table I).

When Davy and Hall[27] added one set of d-functions (the exponent was not given) to their Ca basis set, they observed a bond shortening by ca. 8 pm. However, they did not discuss the large effect. In view of the importance of Ca^{2+}–neutral ligand interactions for biological systems, we have studied these basis set effects for $Ca^{2+}(H_2O)$ by removing or replacing polarization functions on Ca while keeping the same O and H basis sets. The results are summarized in Table III. When the [5d]/(2d) set is replaced by a single d-set (α = 0.986),[41] the Ca–O distance lengthens by ca. 3 pm. Without d-functions or with the diffuse d-function of Ortega-Blake et al.[25] (α = 0.104), we obtain Ca–O distances of ca. 2.35 Å, in agreement with several of the earlier studies (removal of the two 4p-type polarization functions has no significant effect). Thus, at least a DZ d-basis including quite large exponents is needed to obtain reasonable Ca–O distances. This importance of d-functions for metal–ligand distances has been observed previously for various small molecules containing Ca, Sr, or Ba.[50] Moreover, the need for large d-basis sets to obtain correct bending potentials for alkaline-earth-metal MX_2 compounds has been noted by several authors.[51] The large influence of the d-basis on the geometry is due to polarization of the metal

TABLE III: Basis Set Dependency of Equilibrium Geometry, Valence Energy E_{val} (au), and Binding Energy ΔE (kcal/mol) for the Ca^{2+}·H_2O Complex[a]

Ca basis set	Ca–O	O–H	H–O–H	E_{val}	ΔE
[6s6p5d]/(6s6p2d)	2.276	0.954	127.8	−52.913 38	55.6
6s6p1d (α_d = 0.986)	2.307	0.953	128.1	−52.909 27	53.0
6s6p1d (α_d = 0.103)	2.351	0.953	127.9	−52.907 36	51.8
6s6p	2.347	0.952	128.0	−52.907 01	51.6
6s4p	2.348	0.952	128.0	−52.906 86	51.5

[a] Distances in Å, angles in deg. DZ+P and DZP basis sets for O and H, respectively, have been used.

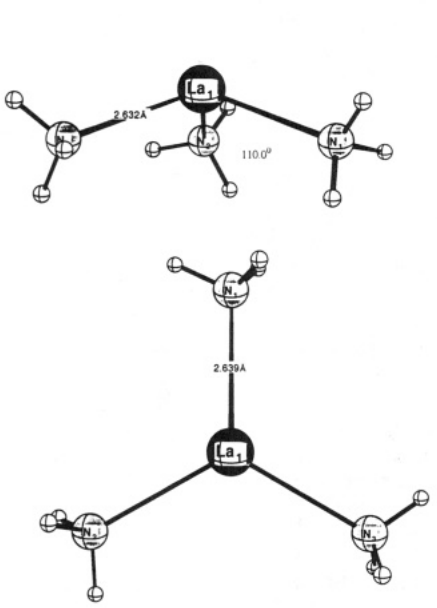

Figure 4. $La^{3+}(NH_3)_3$ geometries. (a) C_3. (b) Planar C_{3h}.

TABLE IV: Effective Ligand Radii (Å) for M^{n+}·L Complexes[a]

M^{n+}	L = H_2O	L = NH_3
K^+	1.27 (−0.10)	1.44 (−0.12)
Rb^+	1.32 (−0.05)	1.50 (−0.06)
Cs^+	*1.37 (0.00)*	*1.56 (0.00)*
Ca^{2+}	1.28 (−0.09)	1.42 (−0.14)
Sr^{2+}	1.27 (−0.10)	1.42 (−0.14)
Ba^{2+}	1.31 (−0.06)	1.41 (−0.15)
Sc^{3+}	1.23 (−0.14)	1.51 (−0.05)
Y^{3+}	1.24 (−0.13)	1.44 (−0.12)
La^{3+}	1.16 (−0.21)	1.36 (−0.20)

[a] The effective ligand radii have been obtained by subtracting tabulated cation radii (cf. ref 51) from the calculated (HF level) M–L distances (cf. Tables I and II). Differences with respect to the values for Cs^+·L are given in parentheses. Note that electron correlation effects shorten the distances by ca. 2–5 pm (cf. Table I).

$(n-1)$-p shell and to small covalent bonding contributions involving metal d-orbitals. These effects have to be included properly into the wave function. The complex binding energy is only slightly lower when inadequate or no d-basis sets are used (cf. Table III). However, we recommend that potential functions used to study heavy alkaline-earth-metal cation binding to biologically relevant ligands should be based on ab initio calculations that reproduce the covalent bonding contributions and the cation polarization correctly.

The MP2 M–O distances in $M^{n+}(H_2O)$ are generally shorter than the HF values by ca. 2.5–4 pm (cf. Table I). This contraction is probably due to the neglect of core-valence correlation in the Hartree–Fock calculations.[1,3,50b-d] The O–H distances show the expected increase by ca. 2 pm at the MP2 level, due to valence correlation. The H–O–H angles are slightly larger at the correlated level. As expected, the deviations of the ligand geometries in the complex from those of the free ligand (probably due to the polarization of the ligand by the positive charge and to charge transfer) increase with increasing cation charge. While, e.g., the O–H distances in the group 1 complexes are only ca. 0.5 pm larger than those in water, the increase with the di- and trications is ca. 1–1.5 and 3–4 pm, respectively. Similar behavior is observed for the increase in the ammonia N-H distances and for the decrease in the H–O–H and H–N–H angles due to complexation (cf. Tables I and II). This charge dependence of ligand deformation is even more pronounced for smaller closed-shell metal cations[19] and for open-shell species.[27]

At the HF level, the M–N(ammonia) distances are larger than the M–O (water) separations by roughly 18, 15, and 13 pm for the group 1, 2, and 3 cations, respectively. This trend indicates an increasing bonding contribution from ligand polarization with increasing metal charge (an effect which is more pronounced for NH_3 than for H_2O[29]). The M–O distances for the alkali metal systems are quite close to those obtained from experimental binding energies by means of a simple electrostatic model[16] (cf. footnotes to Table I). However, the distances for a given ligand do not quite follow the tabulated ionic radii[52] for all cations considered. Assuming the cesium complexes to represent ideal ionic cases, we can obtain an approximate effective ionic radius for the ligand by subtracting the cation radius[52] from the Hartree–Fock bond distance. This effective ligand radius is generally smaller for the other systems (cf. Table IV). This is a further indication that ligand (and cation) polarization effects and small covalent bonding contributions have to be considered, particularly for the trications.

(*b*) *Two-Ligand Complexes.* The O–M–O angles, M–O distances, linearization energies, and bond length changes upon linearization for the complexes $M^{n+}(H_2O)_2$ at the SCF and MP2 levels are summarized in Table V. Table VI gives the corresponding SCF results for the bisammonia complexes.

Obviously, with the exception of the potassium species, all two-ligand complexes favor nonlinear arrangements of the ligands around the cation. While the linearization energies are very small for the quasilinear Rb^+, Cs^+, and Ca^{2+} complexes, the stabilization of the bent structures is significant for the group 3 systems. The Sr and Ba species are intermediate. Most angles are significantly below 180° and, within a given group, decrease with increasing cation radius. Similar trends are known for a large number of Ca, Sr, and Ba MX_2 compounds (X = anionic ligand).[1-6] However, the L–M–L angles in the neutral-ligand complexes are even smaller than the MX_2 X–M–X angles. As observed previously for neutral group 2 MX_2 compounds, the M–L or (M–X) bond lengthens upon linearization.[1,3-6] The geometries obtained by Bauschlicher et al.[36] for $Ca^{2+}(H_2O)_2$ and $Sr^{2+}(H_2O)_2$ agree excellently with our HF results (cf. Table V). In view of the very shallow bending potential, the deviation in the $Ca^{2+}(H_2O)_2$ O–

TABLE V: O–M–O Angles (deg), Linearization Energies ΔE_1 (kcal/mol), M–O Distances (Å), and Bond Lengthening upon Linearization ΔR_1 (Å) for $M^{n+}(H_2O)_2$ Complexes (Hartree–Fock and MP2 Results)

	Hartree–Fock[a]				MP2[b]			
M^{n+}	O–M–O	ΔE_1	R–MO[c]	ΔR_1[c]	O–M–O	ΔE_1	R–MO	ΔR_1
K^+	180.0	0.00	2.692	0.000				
Rb^+	126.3	0.10	2.877	0.009				
Cs^+	113.3	0.26	3.079	0.023	122.0	0.20	3.032	0.020
Ca^{2+}	141.0[d]	0.06[d]	2.312[d]	0.005	143.5	0.18	2.289	0.009
Sr^{2+}	117.5[d]	0.62[d]	2.485[d]	0.020	127.9	0.61	2.462	0.018
Ba^{2+}	109.6	1.03	2.694	0.030	116.8	0.61	2.657	0.025
Sc^{3+}	116.5	3.45	2.024	0.024				
Y^{3+}	112.2	2.99	2.236	0.027				
La^{3+}	107.4	3.73	2.444	0.036	107.0	3.82	2.414	0.040

[a] The most stable (staggered) conformations (C_s, D_{2d}) are compared (cf. Figure 2a,d). [b] The eclipsed C_{2v}^{op} and D_{2h} conformations are compared (cf. Figure 2b,e). Cf. Table VII for the (small) HF rotational barriers. Extended group 2 and La basis sets used. [c] The average of the two nonequivalent (only different by less than 0.005 Å) distances for the C_s structure is given. [d] The Hartree–Fock results of Bauschlicher et al. (cf. ref 36) are O–M–O = 125.5°, R–MO = 2.310 Å, ΔE_1 = 0.3 kcal/mol with Ca^{2+}, and O–M–O = 115.8°, R–MO = 2.489 Å, ΔE_1 = 0.6 kcal/mol with Sr^{2+}.

TABLE VI: N-M-N Angles (deg), Linearization Energies ΔE_1 (kcal/mol), M-N Distances (Å), and Bond Lengthening upon Linearization ΔR_1 (Å) for $M^{n+}(NH_3)_2$ Complexes (Hartree-Fock Results)[a]

M^{n+}	N-M-N	ΔE_1	R-MN	ΔR_1
K^+	180.0	0.00	2.872	0.000
Rb^+	141.8	0.03	2.880	0.006
Cs^+	117.2	0.30	3.268	0.032
Ca^{2+}	132.1	0.37	2.464	0.013
Sr^{2+}	119.4	1.01	2.645	0.030
Ba^{2+}	111.7	1.69	2.855	0.044
Sc^{3+}	117.2	6.37	2.165	0.044
Y^{3+}	113.9	5.91	2.382	0.047
La^{3+}	111.2	7.01	2.594	0.065

[a] Eclipsed C_{2v} and D_{3h} structures are compared (cf. Figure 1).

Ca–O angle is not significant. We have considered different conformations in the Hartree–Fock optimizations of the dihydrate complexes (cf. Figure 2). Except for the K^+ complex which favors a linear D_{2d} geometry, staggered bent C_s structures are the most stable (C_2 structures with twisted ligands are very close in energy to the C_s structures, cf. Table VII). The M–OH_2 rotational barriers are below 0.1 kcal/mol for the alkali-metal complexes, 0.2–0.3 kcal/mol for the alkaline-earth-metal species, and 0.6–0.9 kcal/mol for the group 3 systems (cf. Table VII). These (rather small) conformational preferences differ considerably from those of the isoelectronic $Sr(NH_2)_2$ and $Ba(NH_2)_2$. These diamides have been predicted to prefer in-plane C_{2v} structures (compare Figure 2d) and to exhibit significant M–NH_2 rotational barriers (e.g., ca. 2 kcal/mol per amide group in $Ba(NH_2)_2$), due to $p_\pi \rightarrow d_\pi$ bonding contributions.[4]

Table VIII compares the natural atomic orbital (NAO)[49] metal valence populations for the isoelectronic systems $Ba(NH_2)_2$[4] and $La^{3+}(H_2O)_2$ in different conformations. The linear structures (D_{2d}, D_{2h}) are easiest to analyze: The σ-type populations (d_{z^2} NAOs) are quite similar for the two species. However, the π-type occupations (e.g., d_{xz} and d_{yz} for D_{2d} symmetry) for $La^{3+}(H_2O)_2$ are considerably smaller. π-bonding contributions between the H_2O π-lone-pairs and empty La^{3+} d-orbitals seem to be less favorable than those between NH_2^- π-lone-pairs and the corresponding Ba^{2+} acceptor orbitals in $Ba(NH_2)_2$. In the bent $La^{3+}(H_2O)_2$ structures the La valence populations are generally smaller than for bent $Ba(NH_2)_2$. The ligand-to-metal charge transfer upon bending, that is an inherent feature of heavy group 2 MX_2 compounds,[3,4] is far less pronounced for the La^{3+} dihydrate. In spite of this, the O–La–O angle is only ca. 107°, whereas the N–Ba–N angle in $Ba(NH_2)_2$ is larger (between 118 and 129°, depending on the conformation[4]).

The NPA metal net charges and the metal valence s- and d-populations for the group 2 and 3 dihydrate complexes, in the bent out-of-plane C_{2v} and in the linear D_{2h} structures (cf. Figure 2c,f), are compared in Table IX. Results for the isoelectronic $Ba(NH_2)_2$[4] are again included for comparison. The Sc^{3+} and Y^{3+} complexes have the most covalent character. They exhibit larger metal valence populations than the Ca, Sr, or Ba diamides, dihydroxides, or difluorides.[4] The change in ligand-to-metal charge transfer upon bending is (1) negligible for the practically completely ionic alkali-metal cations (with metal NPA charges between 0.995 and 0.999), (2) is still very small for the group 2 species, but (3) is significant for Sc^{3+}, Y^{3+}, and La^{3+}. The NPA

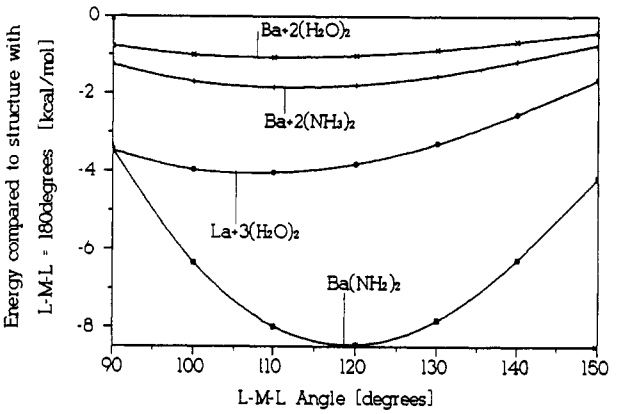

Figure 5. Bending potentials of some cationic $M^{n+}(L)_2$ complexes compared to $Ba(NH_2)_2$, based on HF single-point calculations. Except for the L–M–L angle, all geometry parameters have been kept fixed at their optimized values (within C_s symmetry for $M^{n+}(H_2O)_2$, C_{2v}^{ip} for $Ba(NH_2)_2$, and C_{2v} for $Ba^{2+}(NH_3)_2$; cf. Figures 1 and 2).

populations indicate that the bending of the group 3 species (particularly the Sc^{3+} complexes) is due mainly to d-orbital participation in bonding. The cation polarizabilities increase along the series $Sc^{3+} < Y^+ < La^{3+}$.[53] Therefore, the nonmonotonous trend of the linearization energies (cf. Tables V and VI) cannot be explained purely by cation polarization. On the other hand, the covalent bonding contributions are very small for the alkali-metal complexes. These cations are the most polarizable. Thus, explanations based on cation polarization seem more convincing for the (very small) energy gain upon bending these complexes.

The group 2 compounds are intermediate: The contributions from d-orbital participation in bonding and from cation polarization both may be significant. Covalent bonding contributions *and* cation polarization probably favor bending less strongly in the cationic complex, e.g., in $Ba^{2+}(H_2O)_2$ vs $Ba(NH_2)_2$. However, the factors that oppose bending (ligand–ligand repulsion, π-bonding) are also smaller. Interestingly, the Sr, Ba, and group 3 dihydrates have smaller angles but exhibit lower barriers to linearization than, e.g., the Sr and Ba diamides[4] or dihydrides.[1] Indeed, the bending potentials for the cationic complexes differ considerably from those in the neutral group 2 MX_2 species (cf. Figure 5): While the well at ca. 118° for $Ba(NH_2)_2$ is rather steep,[4] significant repulsion of the ligands sets in at larger angles than, e.g. for $La^{3+}(H_2O)_2$.

The Sr^{2+}, Ba^{2+}, and group 3 bisammonia complexes prefer somewhat larger angles but also significantly larger linearization energies than the dihydrates (cf. Table VI). This apparent contradiction points to a subtle balance between the different factors that control the angles and the depths of the potential wells. Table X summarizes the NPA metal net charges and valence populations for the group 2 and 3 bisammonia complexes. π-bonding contributions are essentially absent. The covalent σ-bonding contributions (cf. d_{yz} NAOs in the bent structures) and the charge transfer upon bending are considerably larger than for the dihydrate complexes (particularly for the group 3 species). This provides a rationalization for the larger linearization energies for the ammonia complexes. The slightly larger angles may be due to the larger ligand size and consequently somewhat increased ligand–ligand repulsion.

TABLE VII: Relative Energies (kcal/mol) and O–M–O Angles (deg) for Different Conformations of $M^{n+}\cdot(H_2O)_2$ Complexes[a,b]

M^{n+}	C_s	C_{2v} (ip)[b]	C_{2v} (op)[b]	C_2	D_{2d}	D_{2h}
Rb^+	0.00 (126.3)		0.07 (136.7)		0.10	0.12
Cs^+	0.00 (113.3)	0.04 (120.2)	0.09 (120.2)	0.00 (114.8)	0.26	0.28
Ca^{2+}	0.00 (141.0)		0.12 (148.5)		0.06	0.19
Sr^{2+}	0.00 (117.5)		0.22 (124.3)		0.62	0.70
Ba^{2+}	0.00 (109.6)	0.07 (115.4)	0.24 (115.1)	0.01 (111.6)	1.03	1.08
Sc^{3+}	0.00 (116.5)	0.21 (120.4)	0.88 (120.7)		3.45	3.82
Y^{3+}	0.00 (112.2)		0.71 (114.9)		2.99	3.21
La^{3+}	0.00 (107.4)	0.03 (108.6)	0.59 (108.6)	–0.01 (110.1)	3.73	3.91

[a] Hartree–Fock results. The bending angles are given in parentheses. [b] Cf. Figure 2 for the different conformations considered.

TABLE VIII: Comparison of NAO Metal Valence Populations for $Ba(NH_2)_2$[a] and $La^{3+}(H_2O)_2$ in Different Conformations[b]

	molecular symmetry[c]				
NAO	C_{2v}^{ip}	C_s	C_{2v}^{op}	D_{2d}	D_{2h}
	(a) $Ba(NH_2)_2$[a]				
6s	0.016	0.015	0.013	0.006	0.006
$5d_{xy}$	0.035	0.046	0.000	0.000	0.000
$5d_{xz}$	0.016	0.020	0.000	0.024	0.042
$5d_{yz}$	0.045	0.008	0.050	0.024	0.000
$5d_{x^2-y^2}$	0.017	0.019	0.021	0.000	0.000
$5d_{z^2}$	0.001	0.014	0.021	0.021	0.022
$5d_{tot}$	0.114	0.107	0.092	0.069	0.064
	(b) $La^{3+}(H_2O)_2$				
6s	0.008	0.009	0.008	0.005	0.005
$5d_{xy}$	0.014	0.028	0.001	0.000	0.000
$5d_{xz}$	0.007	0.007	0.000	0.011	0.020
$5d_{yz}$	0.027	0.004	0.029	0.011	0.001
$5d_{x^2-y^2}$	0.013	0.011	0.017	0.000	0.000
$5d_{z^2}$	0.001	0.011	0.014	0.025	0.025
$5d_{tot}$	0.062	0.061	0.061	0.047	0.046

[a] See ref 4. [b] The valence p populations generally are very small. [c] Note that the assignment of coordinate axes is different for C_{2v}, C_s, D_{2d}, and D_{2h} symmetries (cf. Figure 2).

TABLE IX: NPA Metal Net Charges and Valence Populations for the Group 2 and 3 Dihydrate Complexes and $Ba(NH_2)_2$[a]

		Q	s	d_{xy}	d_{xz}	d_{yz}	$d_{x^2-y^2}$	d_{z^2}
Ca^{2+}	C_{2v}	1.975	0.010			0.006	0.006	0.002
	D_{2h}	1.976	0.010		0.006			0.009
Sr^{2+}	C_{2v}	1.982	0.007			0.006	0.005	0.002
	D_{2h}	1.985	0.006		0.004			0.007
Ba^{2+}	C_{2v}	1.987	0.004			0.007	0.004	0.002
	D_{2h}	1.990	0.002		0.004			0.002
Sc^{3+}	C_{2v}	2.789	0.027	0.005	0.002	0.082	0.057	0.037
	D_{2h}	2.816	0.022		0.065	0.006		0.088
Y^{3+}	C_{2v}	2.888	0.020	0.001	0.001	0.044	0.025	0.021
	D_{2h}	2.905	0.015		0.033	0.002		0.044
La^{3+}	C_{2v}	2.937	0.009	0.001		0.029	0.017	0.014
	D_{2h}	2.950	0.005		0.020	0.001		0.025
$Ba(NH_2)_2$	C_{2v}	1.894	0.013			0.050	0.021	0.021
	D_{2h}	1.933	0.006		0.042			0.022

[a] Data for the bent out-of-plane C_{2v} and the linear D_{2h} structures are given (cf. Figure 2c,f, respectively). Blanks indicate populations below 0.0005. Note that the assignment of coordinate axes is different for C_{2v} and D_{2h} symmetries (see Figure 2). The charges do not exactly match 2 minus the sum of the populations, as the small p-populations and some small contributions from Rydberg NAOs have been neglected.

All M–O and M–N distances in the two-ligand complexes are slightly (ca. 3–5 pm) longer than those in the single-ligand species. This probably is due to ligand–ligand repulsion[35] and to screening of the positive charge by the second ligand. The ligand geometries are practically identical in the one- and two-ligand systems. Only the Sc^{3+} complexes exhibit a slight decrease of the N–H and O–H bond lengths (by ca. 1 pm in the two-ligand systems); with Y^{3+} and La^{3+} the difference already is as small as 0.5 pm. This indicates moderate charge-screening by the second ligand. Some of the water complexes have been optimized at the MP2 level of theory. As these calculations were restricted to the C_{2v} (out-of-plane) and D_{2h} structures (cf. Figure 2c,f), the angles and relative energies should be compared to the SCF results for the same symmetries (cf. Table VII). Apparently, the effect of correlation on the angular geometries and linearization energies is small. This was observed previously for neutral group 2 MX_2 compounds.[1,3,51] The M–O distances decrease and the O–H distances increase upon inclusion of correlation corrections (cf. above for the single-ligand complexes).

(c) *Three-Ligand Complexes.* As we expect most of the structural trends observed above for the two-ligand complexes to be transferable to higher coordination numbers, we have restricted our investigation of three-ligand systems to some Ba^{2+} and La^{3+} species (cf. ref 36 for the structure of $Sr^{2+}(H_2O)_3$). In these cases we expect the largest deviations from regular (planar) structures within the sets of group 2 and 3 complexes, respectively. The linearization energies for Rb^+ or Cs^+ two-ligand complexes are very small. Thus, we do not expect any significant deviation from planarity in the alkali-metal cation three-ligand species.

TABLE X: NPA Metal Net Charges and Valence Populations for the Group 2 and 3 Bisammonia Complexes[a]

		Q	s	d_{xy}	d_{xz}	d_{yz}	$d_{x^2-y^2}$	d_{z^2}
Ca^{2+}	C_{2v}	1.937	0.041	0.001		0.008	0.009	0.002
	D_{3h}	1.943	0.036		0.001			0.015
Sr^{2+}	C_{2v}	1.950	0.029	0.001		0.011	0.007	0.001
	D_{3h}	1.959	0.024		0.001	0.001		0.014
Ba^{2+}	C_{2v}	1.961	0.017	0.001		0.014	0.008	0.001
	D_{3h}	1.970	0.012		0.001			0.015
Sc^{3+}	C_{2v}	2.693	0.078	0.006	0.002	0.141	0.074	0.006
	D_{3h}	2.772	0.064		0.007	0.007		0.144
Y^{3+}	C_{2v}	2.815	0.061	0.002	0.001	0.079	0.040	0.002
	D_{3h}	2.865	0.045		0.003	0.003		0.079
La^{3+}	C_{2v}	2.874	0.029	0.002	0.001	0.064	0.032	0.002
	D_{3h}	2.914	0.017		0.004	0.004		0.058

[a] Cf. Figure 1 for the geometries and standard orientations. Blanks indicate populations below 0.0005. Note, that the assignment of coordinate axes is different for C_{2v} and D_{3h} symmetries (see Figure 1). The charges do not exactly match 2 minus the sum of the populations, as the small p-populations and some small contributioins from Rydberg NAOs have been neglected.

TABLE XI: Geometries and Relative Energies (kcal/mol) of Some Three-Ligand Complexes of Ba^{2+} and La^{3+} in Different Conformations[a]

(a) $Ba^{2+}(H_2O)_3$			
structure	Ba–O	O–Ba–O	E_{rel}
C_3	2.734	89.2	0.00
C_{3v}(ip)[b]	2.742	119.5	0.56
C_{3v}(op)[b]	2.734	116.2	0.74
D_3	2.742	120	0.38
D_{3h}(ip)[b]	2.742	120	0.56
D_{3h}(op)[b]	2.745	120	0.76
(b) $La^{2+}(H_2O)_3$			
structure	La–O	O–La–O	E_{rel}
C_3	2.470	107.8	0.00
C_{3v}(ip)[b]	2.472	116.9	0.36
C_{3v}(op)[b]	2.474	108.2	1.16
D_3	2.474	120	0.39
D_{3h}(ip)[b]	2.473	120	0.39
D_{3h}(op)[b]	2.484	120	2.05
(c) $La^{3+}(NH_3)_3$			
structure	La–N	N–La–N	E_{rel}
C_3	2.632	110.0	0.00
C_{3h}	2.639	120	0.76

[a] Distances in Å, angles in deg. [b] Two different D_{3h} structures, with the hydrogen atoms either in the plane of the heavy atoms (D_{3h}(ip)) or perpendicular to it (D_{3h}(op)), as well as the corresponding C_{3v} geometries obtained after pyramidalization (cf. Figure 3c,d), have been considered.

The complexes $M^{n+}(H_2O)_3$ (M^{n+} = Ba^{2+}, La^{3+}) indeed prefer pyramidal C_3 structures (the water molecules are twisted to minimize repulsion, cf. Figure 3a). The energy gain with respect to the corresponding planar D_3 geometries (cf. Figure 3b) is ca. 0.4 kcal/mol for both species (cf. Table XI). C_{3v} structures with eclipsed water molecules (cf. Figure 3c,d) or planar D_{3h} geometries are generally higher in energy. Interestingly, the C_{3v} structures with the H–O–H plane containing the C_3 axis (cf. Figure 3c) are lower in energy than the out-of-plane C_{3v} geometries (cf. Figure 3d), but they are less pyramidalized (cf. Table XI). This may be due to π-bonding contributions. $La^{3+}(HF)_3$ and $La^{+}(NH_3)_3$ also exhibit nonplanar geometries (cf. Tables XI and XII). The planarization energy increases in the order $La^{3+}(HF)_3$ < $La^{3+}(H_2O)_3$ < $La^{3+}(NH_3)_3$, but the L–La–L angles increase in

TABLE XII: Geometries and Relative Energies (kcal/mol) for Different Conformations of Complexes $La^{3+}(HF)_m$ (m = 1-3)[a]

	La-F	F-La-F	E_{rel}
(a) $La^{3+}(HF)$			
	2.383		
(b) $La^{3+}(HF)_2$			
C_2	2.405	105.6	0.00
C_{2h}	2.425	180	1.25
(c) $La^{3+}(HF)_3$			
C_{3v}	2.425	104.8	0.00
D_{3h}	2.430	120	0.25

[a] Distances in Å, angles in deg.

TABLE XIII: Ligand Binding Energies $-\Delta E$ (kcal/mol) in Complexes $M^{n+}(H_2O)_m$

	ΔE					
	m = 1			m = 2		
M^{n+}	HF	MP2[a]	MP4[a,b]	HF[c]	MP2[a,d]	$\Delta\Delta E_{12}$(HF)[e]
K^+	19.1[f]	19.6[f]		17.1		2.1
Rb^+	16.9[f]	17.4[f]		15.1		1.4
Cs^+	14.8[f]	15.5[f]		13.2	13.9	1.6
Ca^{2+}	55.6[g]	58.1	57.7	50.0[g]	51.7	5.6
Sr^{2+}	47.4[g]	49.7	49.3	42.8[g]	44.4	4.6
Ba^{2+}	40.0	42.3	41.9	36.3	38.0	3.7
Sc^{3+}	130.3	141.2		107.8		22.5
Y^{3+}	101.9	109.9		88.8		13.1
La^{3+}	82.1	87.8		72.9	75.7	9.2

[a] Correlated calculations used extended group 2 and 3 basis sets. [b] MP4SDTQ single points at MP2-optimized geometries. [c] Based on C_s geometry of $M^{n+}(H_2O)_2$ (cf. Figure 2a). [d] Based on C_{2v}[op] geometry of $M^{n+}(H_2O)_2$ (cf. Figure 2c). Note that the barriers to M-OH_2 rotation are negligible compared to the binding energies. [e] Hartree-Fock difference between first and second ligand binding energy. [f] The experimental $\Delta H°$ values for first (second) ligand binding are 17.9 (16.1), 15.9 (13.6), 13.7 (12.5) kcal/mol with K^+, Rb^+, and Cs^+, respectively (cf. ref 16). [g] The Hartree-Fock values obtained by Bauschlicher et al. (cf. ref 36) are 55.0, 48.9, 46.9, and 42.0 kcal/mol for $Ca^{2+}(H_2O)$, $Ca^{2+}(H_2O)_2$, $Sr^{2+}(H_2O)$, and $Sr^{2+}(H_2O)_2$, respectively.

the same direction. This is the same trend observed for the two-ligand complexes (cf. discussion above).

(B) Ligand Binding Energies. Tables XIII and XIV summarize the first and second ligand binding energies for the hydrate and ammonia complexes, respectively. As expected for electrostatic reasons, the ligand binding energies (for a given number and type of ligands) increase considerably with the metal charge. For a given charge these energies decrease with increasing cation size. Electron correlation corrections have been considered for the water complexes. Correlation leads to slightly larger binding energies. This effect is largest for the trications. The increase is due to the reduction of metal core-valence repulsion at the correlated level. MP2 single point calculations at the SCF-optimized geometries yield binding energies that are practically identical to those obtained with MP2 optimized structures. Although the MP2 bond lengths are shorter, the effect on the binding energies is small, due to the very shallow M-O potential curves.

The calculated binding energies ΔE for the group 1 complexes with water and ammonia differ by less than 2 kcal/mol from the corresponding experimental $\Delta H°$ values[16,17] (cf. footnotes in Tables XIII and XIV). Comparison with other theoretical results confirms the observations made for the metal-ligand distances (cf. section A): Ligand basis sets that are too small lead to an overestimation of ligand binding, due to BSSE.[23,29] The omission of compact d-functions on Ca^{2+} and Sr^{2+} leads to slightly small binding energies[22,25,28,31,32] (cf. Table III). The results of Bauschlicher et al.[36] for Ca^{2+} and Sr^{2+} are in good agreement with our HF values (cf. Table XIII).

The binding energy of the second ligand is smaller than that of the first. The difference increases with metal charge and decreases with cation size (cf. Tables XIII and XIV). The same effects (charge screening by the second ligand and ligand-ligand repulsion) cause the increase of the M-L distances (cf. section A). The ammonia binding energies for the group 2 and 3 cations are larger than the corresponding water binding energies, particularly for the trications. This agrees with previous studies[21,29,34c] and is due to the fact that the ammonia dipole moment is located closer to the cation than the water dipole.[34c] In most cases, the differences ΔE_{12} (cf. Tables XIII and XIV) are also larger with ammonia (cf. refs 35 and 36).

TABLE XIV: Ammonia Binding Energies $-\Delta E_m$ (kcal/mol) for $M^{n+}(NH_3)_m$ Complexes[a]

M^{n+}	ΔE_1	ΔE_2	$\Delta\Delta E_{12}$[b]
K^+	19.6[c]	17.1	2.5
Rb^+	17.0[c]	14.9	2.1
Cs^+	14.8	12.9	1.9
Ca^{2+}	62.4	54.1	8.3
Sr^{2+}	52.4	45.9	6.5
Ba^{2+}	43.5	38.5	5.0
Sc^{3+}	151.4	118.8	32.6
Y^{3+}	117.4	98.5	18.9
La^{3+}	94.0	82.7	11.3

[a] Hartree-Fock results. [b] Difference between first and second ligand binding energy. [c] The experimental $\Delta H°$ values for first(second) ligand binding are 20.1 (16.3) and 18.7 (15.2) kcal/mol with K^+ and Rb^+, respectively (cf. ref 17).

Conclusions

Complexes of the group 2 and 3 cations Sr^{2+}, Ba^{2+}, Sc^{3+}, Y^{3+}, and La^{3+} (which all have a formal noble-gas electronic configuration) with two neutral ligands such as NH_3, H_2O, or HF favor a bent coordination of the cation. Even Ca^{2+}, Rb^+, and Cs^+ complexes are quasilinear and exhibit deviations from linearity. The calculated linearization energies vary from very small (<0.2 kcal/mol for Rb^+ complexes) to rather large values (ca. 7 kcal/mol for $La^{3+}(NH_3)_2$). Three-ligand Ba^{2+}, La^{3+} and Sr^{2+} [36] systems, and probably also of those of Sc^{3+} and Y^{3+}, favor pyramidal geometries. Their planarization barriers are considerably smaller than the corresponding linearization energies of the two-ligand complexes.

The predicted bending angles for the $M^{n+}L_2$ species are smaller than those calculated previously for neutral MX_2 species (M = Ca, Sr, Ba, lanthanide (II)).[1-6,13c] Likewise, the F-La-F angle for the three-ligand complex $La^{3+}(HF)_3$ is smaller than that found for LaF_3.[13c] These small angles are due to the considerably reduced repulsion between the neutral ligands compared to the Coulomb-type repulsion between anions. Additionally, π-bonding (which tends to favor linear or planar structures[4,11]) seems to be less favorable in the cation-neutral ligand complexes. On the other hand, the factors that favor bent (or pyramidal) structures (covalent σ-type bonding contributions involving metal d-orbitals, and the polarization of the cation by the ligands)[1,3] also seem to be reduced in the cationic complexes. Due to these counteracting effects, the characteristics of the bending (or pyramidalization) potentials may be quite different from those found for the corresponding neutral species (smaller angles may be combined with smaller linearization energies).

Accurate ab initio calculations on complexes of Ca^{2+}, Sr^{2+}, or Ba^{2+}, important for studies of biologically relevant systems, require extended d-basis sets of at least DZ quality including large exponents.

Acknowledgment. This work was supported by the Deutsche Forschungsgemeinschaft, the Fonds der Chemischen Industrie, the Stiftung Volkswagenwerk, and Convex Computer Corporation. M.K. acknowledges a Kekulé grant by the Fonds der Chemischen Industrie. We are grateful to Prof. H. Preuss and the theoretical chemistry group in Stuttgart for providing pseudopotentials and valence basis sets prior to publication (cf. refs 39 and 43) and to Prof. H. Stoll (Stuttgart) for helpful discussions. We also thank Dr. C. W. Bauschlicher, Jr. (NASA Ames Research Center) for sending us a preprint of ref 36.

Supplementary Material Available: Harmonic vibrational frequencies and force constants obtained at the Hartree-Fock level

of theory for ScF_3, YF_3, LaF_3, $Ca^{2+}\cdot H_2O$, and $Sc^{3+}\cdot H_2O$ (2 pages). Ordering information is given on any current masthead page.

References and Notes

(1) Kaupp, M.; Schleyer, P. v. R.; Stoll, H.; Preuss, H. *J. Chem. Phys.* **1991**, *94*, 1360.

(2) Seijo, L.; Barandiaran, Z.; Huzinaga, S. *J. Chem. Phys.* **1991**, *94*, 3762.

(3) Kaupp, M.; Schleyer, P. v. R.; Stoll, H.; Preuss, H. *J. Am. Chem. Soc.* **1991**, *113*, 6012.

(4) Kaupp, M.; Schleyer, P. v. R. *J. Am. Chem. Soc.* **1992**, *114*, 491.

(5) Kaupp, M.; Schleyer, P. v. R. Dolg, M.; Stoll, H. *J. Am. Chem. Soc.*, in press.

(6) Mösges, G.; Hampel, F.; Kaupp, M.; Schleyer, P. v. R., submitted to *J. Am. Chem. Soc.*

(7) Büchler, A.; Stauffer, J. L.; Klemperer, W.; Wharton, L. *J. Chem. Phys.* **1963**, *39*, 2299.

(8) Beattie, L. R.; Jones, P. J.; Young, N. A. *Angew. Chem.* **1989**, *101*, 322. Beattie, L. R.; Jones, P. J.; Young, N. A. *Angew. Chem., Int. Ed. Engl.* **1989**, *28*, 13.

(9) (a) Cotton, F. A.; Wilkinson, G. *Advanced Inorganic Chemistry*, 5th ed.; Wiley: New York, 1988. (b) Gillespie, R. J.; Hargittai, I. *The VSEPR Model of Molecular Geometry*; Allyn and Bacon: Boston, 1991.

(10) Guido, M.; Gigli, G. *J. Chem. Phys.* **1976**, *65*, 1397.

(11) Jolly, C. A.; Marynick, D. S. *Inorg. Chem.* **1989**, *28*, 2893.

(12) Ghotra, J. S.; Hursthouse, M. B.; Welch, A. J. *J. Chem. Soc., Chem. Commun.* **1973**, 669. Andersen, R. A.; Templeton, D. H.; Zalkin, A. *Inorg. Chem.* **1978**, *17*, 2317.

(13) (a) Yates, J. H.; Pitzer, R. M. *J. Chem. Phys.* **1979**, *70*, 4049 (ScF_3). (b) Hartree–Fock geometry optimization for YF_3 with the Y and F pseudopotentials and basis sets used in this work gives a planar D_{3h} structure with R–YF = 2.026 Å. The harmonic vibrational frequencies and force constants calculated for ScF_3, YF_3, and LaF_3 are available as supplementary material. (c) Dolg, M.; Stoll, H.; Preuss, H. *THEOCHEM* **1991**, *235*, 67.

(14) (a) Conway, B. E. *Ionic Hydration in Chemistry and Biophysics*; Elsevier: New York, 1982. (b) Schuster, P.; Jakubetz, W.; Marius, W. *Top. Curr. Chem.* **1975**, *60*, 1. (c) Hunt, J. P.; Friedman, H. L. *Adv. Inorg. Chem.* **1983**, *30*, 359. (d) Kebarle, P. *Annu. Rev. Phys. Chem.* **1977**, *28*, 445. (e) Freiser, B. S.; Beauchamp, J. L. *J. Am. Chem. Soc.* **1977**, *99*, 3214. (f) Castleman Jr., A. W.; Tang, I. N.; Munkelwitz, H. R. *Science* **1971**, *173*, 1025.

(15) Narcisi, R. S.; Bailey, A. D. *J. Geophys. Res.* **1965**, *70*, 3687. Hayhurst, A. N.; Sugden, T. M. *Proc. R. Soc. London* **1966**, *A293*, 36.

(16) Dzidić, I.; Kebarle, P. *J. Phys. Chem.* **1970**, *74*, 1466.

(17) Castleman Jr., A. W.; Holland, P. M.; Lindsay, D. M.; Peterson, K. I. *J. Am. Chem. Soc.* **1978**, *100*, 6039. Castleman Jr., A. W. *Chem. Phys. Lett.* **1978**, *53*, 560.

(18) Blades, A. T.; Jayaweera, P.; Ikonmou, M. G.; Kebarle, P. *J. Chem. Phys.* **1990**, *92*, 5900.

(19) For literature coverage through 1974, see ref 14b. Diercksen, G. H. F.; Kraemer, W. P.; Roos, B. O. *Theor. Chim. Acta* **1975**, *36*, 249. Woodin, R. L.; Houle, F. A.; Goddard III, W. A. *Chem. Phys.* **1976**, *14*, 461. Corongiu, G.; Clementi, E. *J. Chem. Phys.* **1978**, *69*, 4885. Clementi, E.; Kistenmacher, H.; Kolos, W.; Romano, S. *Theor. Chim. Acta* **1980**, *55*, 257. Del Bene, J. E.; Frisch, M. J.; Raghavachari, K.; Pople, J. A.; Schleyer, P. v. R. *J. Phys. Chem.* **1983**, *87*, 73. Del Bene, J. E.; Mettee, H. D.; Frisch, M. J.; Luke, B. T.; Pople, J. A. *J. Phys. Chem.* **1983**, *87*, 3279. Hermansson, K.; Olovsson, I.; Lunall, S. *Theor. Chim. Acta* **1984**, *64*, 265. Probst, M. M. *Chem. Phys. Lett.* **1987**, *137*, 229. Latajka, Z.; Scheiner, S. *J. Chem. Phys.* **1987**, *87*, 1194. Probst, M. M. *Theochem* **1990**, *208*, 45. Bauschlicher, C. W.; Langhoff, S. R.; Partridge, H.; Rice, J. E.; Komornicki, A. *J. Chem. Phys.* **1991**, *95*, 5142.

(20) Kistenmacher, H.; Popkie, H.; Clementi, E. *J. Chem. Phys.* **1973**, *58*, 1689.

(21) Berthod, H.; Pullman, A. *Chem. Phys. Lett.* **1980**, *70*, 434.

(22) Kollman, P. A.; Kuntz, I. D. *J. Am. Chem. Soc.* **1972**, *94*, 9236.

(23) Pullman, A.; Berthod, H.; Gresh, N. *Int. J. Quant. Chem. Symp.* **1976**, *10*, 59.

(24) Kochanski, E.; Prissette, J. *Chem. Phys. Lett.* **1981**, *80*, 564.

(25) Ortega-Blake, I.; Barthelat, J. C.; Costes-Puech, E.; Oliveros, E.; Daudey, J. P. *J. Chem. Phys.* **1982**, *76*, 4130. Ortega-Blake, I.; Hernandez, J.; Novaro, O. *J. Chem. Phys.* **1984**, *81*, 1894.

(26) Ortega-Blake, I.; Novaro, O.; Lés, A.; Rybak, S. *J. Chem. Phys.* **1982**, *76*, 5404.

(27) Davy, R. D.; Hall, M. B. *Inorg. Chem.* **1988**, *27*, 1417.

(28) Cachau, R. E.; Villar, H. O.; Castro, E. A. *Theor. Chim. Acta* **1989**, *75*, 299.

(29) Hofmann, H.-J.; Hobza, P.; Cammi, R.; Tomasi, J.; Zahradnik, R. *THEOCHEM* **1989**, *201*, 339.

(30) Bruning, H.; Feil, D. *J. Chem. Phys.* **1989**, *91*, 1121.

(31) Krauss, M.; Stevens, W. J. *J. Am. Chem. Soc.* **1990**, *112*, 1460.

(32) Shiratori, Y.; Setsuko, N. *J. Comput. Chem.* **1991**, *12*, 717.

(33) For some studies involving other model ligands see, e.g.: Ortega-Blake, I.; Lés, A.; Rybak, S. *J. Theor. Biol.* **1983**, *104*, 571. Maynard, A. T.; Hiskey, R. G.; Pedersen, L. G.; Koehler, K. A. *Theochem* **1985**, *124*, 213. Hori, K.; Kushick, J. N.; Weinstein, H. *Biopolymers* **1988**, *27*, 1865.

(34) (a) Bauschlicher Jr., C. W.; Langhoff, S. R. *Int. Rev. Phys. Chem.* **1990**, *9*, 149. (b) Bauschlicher Jr., C. W.; Langhoff, S. R.; Partridge, H. *J. Chem. Phys.* **1990**, *94*, 2068. (c) Langhoff, S. R.; Bauschlicher, C. W.; Partridge, H.; Sodupe, M. *J. Phys. Chem.* **1991**, *95*, 10677. (d) For a study of the bonding of Sc, Y, and La mono- and dications to small hydrocarbons, see: Bauschlicher Jr., C. W.; Langhoff, S. R. *J. Chem. Phys.* **1991**, *95*, 2278.

(35) Bauschlicher, C. W.; Partridge, H. *J. Phys. Chem.* **1991**, *95*, 3946. Bauschlicher, C. W.; Partridge, H. *Chem. Phys. Lett.* **1991**, *181*, 129. Sodupe, M.; Bauschlicher, C. W. *Chem. Phys. Lett.* **1991**, *181*, 321.

(36) Bauschlicher Jr., C. W.; Sodupe, M.; Partridge, H. *J. Chem. Phys.* **1992**, *96*, 4453. We thank Dr. C. W. Bauschlicher Jr. for a preprint of this work.

(37) Küchle, W.; Bergner, A.; Dolg, M.; Stoll, H.; Preuss, H., to be published.

(38) Dolg, M.; Wedig, U.; Stoll, H.; Preuss, H. *J. Chem. Phys.*, **1987**, *86*, 866.

(39) Andrae, D.; Häussermann, U.; Dolg, M.; Stoll, H.; Preuss, H. *Theor. Chim. Acta* **1990**, *77*, 123.

(40) Dolg, M.; Stoll, H.; Savin, A.; Preuss, H. *Theor. Chim. Acta* **1989**, *75*, 173. Dolg, M.; Stoll, H. *Theor. Chim. Acta* **1989**, *75*, 369.

(41) Huzinaga, S., Ed. *Gaussian Basis Sets for Molecular Calculations*; Elsevier: New York, 1984.

(42) Igel-Mann, G.; Stoll, H.; Preuss, H. *Mol. Phys.* **1988**, *65*, 1321.

(43) Dolg, M. Dissertation, Universität Stuttgart, 1989.

(44) Poppe, J.; Igel-Mann, G.; Savin, A.; Stoll, H., unpublished results.

(45) Clark, T.; Chandrasekhar, J.; Spitznagel, G. W.; Schleyer, P. v. R. *J. Comput. Chem.* **1983**, *4*, 294.

(46) Dunning, T. H.; Hay, P. J. In *Methods of Electronic Structure Theory*; Schaefer III, H. F., Plenum Press: New York, 1977; Modern Theoretical Chemistry, Vol. 3 p 1.

(47) GAUSSIAN 88; Frisch, M. J.; Head-Gordon, M.; Schlegel, H. B.; Raghavachari, K.; Binkley, J. S.; Gonzalez, C.; DeFrees, D. J.; Fox, D. J.; Whiteside, R. A.; Seeger, R.; Melius, C. F.; Baker, J.; Kahn, L. R.; Stewart, J. J. P.; Fluder, E. M.; Topiol, S.; Pople, J. A.; Gaussian, Inc.: Pittsburgh, PA, 1988.

(48) GAUSSIAN 90, Revision F, Frisch, M. J.; Head-Gordon, M.; Trucks, G. W.; Foresman, J. B.; Schlegel, H. B.; Raghavachari, K.; Robb, M.; Binkley, J. S.; Gonzalez, C.; DeFrees, D. J.; Fox, D. J.; Whiteside, R. A.; Seeger, R.; Melius, C. F.; Baker, J.; Kahn, L. R.; Stewart, J. J. P.; Topiol, S.; Pople, J. A.; Gaussian, Inc.: Pittsburgh, PA, 1990.

(49) Reed, A. E.; Weinstock, R. B.; Weinhold, F. *J. Chem. Phys.* **1985**, *83*, 735. Reed, A. E.; Weinhold, F. *J. Chem. Phys.* **1985**, *83*, 1736. Reed, A. E.; Curtiss, L. A.; Weinhold, F. *Chem. Rev.* **1988**, *88*, 899.

(50) (a) Pyykkö, P. *J. Chem. Soc., Faraday Trans. 2* **1979**, *75*, 1256. (b) Jeung, G.; Daudey, J.-P.; Malrieu, J.-P. *Chem. Phys. Lett.* **1983**, *98*, 433. (c) Pettersson, L. G. M.; Siegbahn, P. E. M.; Ismail, S. *Chem. Phys.* **1983**, *82*, 355. (d) Partridge, H.; Bauschlicher, C. W.; Walch, S. P.; Liu, B. *J. Chem. Phys.* **1983**, *72*, 1866.

(51) See refs 1–3 for discussions and further literature.

(52) Shannon, R. D. *Acta Crystallogr.* **1976**, *A32*, 751.

(53) Schmidt, P. C.; Weiss, A.; Das, T. P. *Phys. Rev. B* **1979**, *19*, 5525.